I&EC research
Industrial & Engineering Chemistry Research

ARTICLE

pubs.acs.org/IECR

Synergy Pinch Analysis of CO_2 Desorption Process

Yun S. Yu,[†] Yun Li,[‡] Hong F. Lu,[†] Rui F. Dong,[†] Zao X. Zhang,*[,†,‡] and Xiao Feng[†,‡]

[†]State Key Laboratory of Multiphase Flow in Power Engineering and [‡]School of Energy and Power Engineering, Xi'an Jiaotong University, No. 28 Xianning West Road, Xi'an 710049, P.R. China

Supporting Information

ABSTRACT: To reduce the regeneration costs of capturing CO_2 with absorbents, a two-dimensional desorption model for two-phase flow has been proposed. The temperature and pressure predicted by the model were found to agree well with the experiment data. A new synergy pinch concept was proposed to determine the interactive synergy impacts on mass and heat transfer. According to the proposed synergy pinch principle, the carbon surplus (SAC) and energy surplus (SAE) were defined to quantify the synergy effects for mass and heat transfer, respectively. The proposed synergy pinch principle is that the lower the values of SAC and SAE, the more effective the CO_2 desorption. In addition, the synergy pinch point can be identified at the ideal value of zero SAC and SAE. Based on this analysis, a stripper with fin internals was introduced that could contribute energy savings of about 10−14% by synergizing the fluid flow between mass and heat transfer. Thus, it was verified that the synergy pinch method can be effectively applied in CO_2 emissions control.

1. INTRODUCTION

Emissions of greenhouse gases such as CO_2 have attracted interest from many countries and organizations throughout the world. Among the industrial capture processes used in China, chemical absorption of CO_2 distinguishes itself by exhibiting a large capture capacity, high rate, and long-term stability. However, the enormous energy consumption has blocked its path to large-scale industrialization. To achieve economic feasibility, attention must be paid to the regeneration part of the capture system, as the main thermal regeneration resistance is encountered in the stripper. As for the absorption of CO_2, mass and heat transfer together with reversible reaction processes coexist during the desorption process. In this sense, more efforts should be focused on coupled effects under multiprocess conditions. Complete and precise modeling is intended to demonstrate the complicated physical mechanism in the multiple processes of CO_2 desorption. With substantial knowledge of the coupled mechanism, process intensification is one way to reduce the cost of CO_2 desorption. This work attempts to achieve lower energy costs in the desorption of CO_2 by a proposed synergy pinch theory.

Regeneration modeling has been studied widely in gas separation. In this field, mass transfer together with transient state dynamics were first successfully investigated by applying the gas-phase film and liquid-phase Higbie penetration model.[1,2] However, the one-dimensional structure and small study range prevented the development of the model because only the macrocopic stripper unit was investigated without including the full internal mechanism of the separation process. Therefore, the mass-transfer model was redeveloped according to rigorous rate-based steady-state conditions, exhibiting interface heat and mass transfer coupled with chemical reaction. Following this achievement, two-phase flow effects were investigated in depth. However, the resulting complicated nonlinear algebraic equations cannot clearly present the coupled effects due to the involved dynamics.[3−6] Later, an intense study of a regeneration system incorporating a stripper, a reboiler, and a heat exchanger system was reported. An equilibrium model was employed to simplify the desorption process at this stage.[7−10] The latest work using Aspen Custom Modeler focused on the integration of the absorption and desorption processes, but the results did not seem satisfactory because they relied on empirical experimental correlations.[11] All of the works mentioned above revealed some useful knowledge about the CO_2 desorption system to a certain extent. However, sufficient specified information on CO_2 desorption that can accurately illustrate the evolution of CO_2 generation upon thermal regeneration is still lacking. This work accounts for CO_2 desorption from coupled gas- and liquid-phase effects to improve the capture efficiency through process intensification. It is anticipated that the two-phase flow model will be more reasonable to describe coupled effects in the regeneration process.

Based on the desorption model, a key problem is how to increase the amount of regeneration and reduce the energy consumption. Herein, a synergy pinch theory, as depicted in Figure 1, is proposed to solve the problem. Hopefully, the field synergy analysis can demonstrate the phenomenon in the desorption process by referencing its application in CO_2 absorption.[12−14] Because the previous field synergy analysis for the absorption process achieved a high capture efficiency, the possibility of intensifying the regeneration process by synergy analysis is promising because of the similarities between absorption and desorption. The field synergy principle can find the bottleneck in coupled effects and identify a way to intensify CO_2 desorption by studying the field distributions. In addition, pinch theory is also an integrated approach to energy and mass conservation, especially the hydrogen pinch method, which has been used extensively in the chemical field.[15−21] The research aim for the CO_2 desorption system is similar to that for hydrogen systems used in the

Received: March 10, 2011
Accepted: November 3, 2011
Revised: September 8, 2011
Published: November 03, 2011

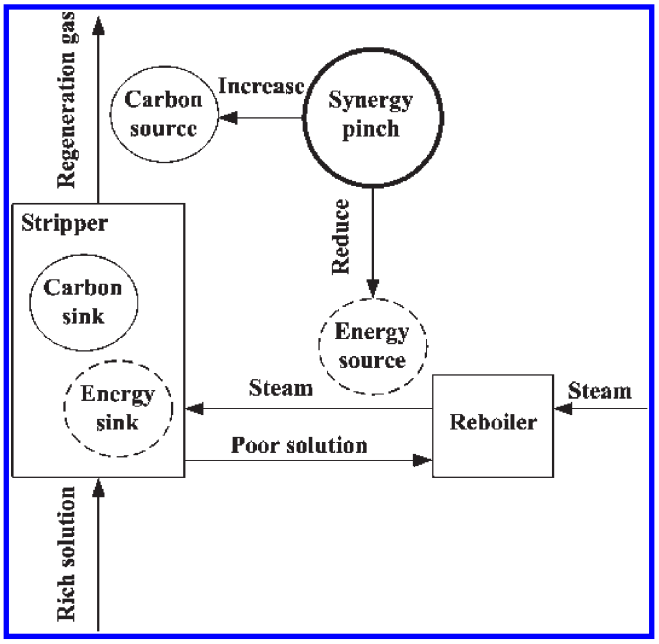

Figure 1. Schematic of synergy pinch in the CO_2 desorption system.

chemical industry. The former aims to make use of utilities efficiently (large amounts of regenerated CO_2 and steam), whereas the latter focuses on highly efficient use of hydrogen. Thus, the method of hydrogen pinch can be extended to the CO_2 desorption process to optimize the coupled fields achieved by field synergy analysis. Therefore, it is possible to integrate field synergy and hydrogen pinch to form a synergy pinch. It is anticipated that this integration theory can take advantage of the intensification traits of the two methods to achieve optimal desorption conditions. Under these circumstances, the synergy pinch point is expected to keep the amount of regeneration CO_2 as large as possible and to make energy consumption as small as possible.

The synergy pinch theory is established for the proposed carbon surplus (SAC) and energy surplus (SAE) variables, which can be obtained by field synergy analysis for the two-phase flows in CO_2 desorption. Synergy pinch graphs are presented herein with reference to the method used in the hydrogen pinch system.[22−24] The hydrogen pinch method has been widely applied to minimize the hydrogen utility in chemical systems. The effective improvements obtained by this method for hydrogen systems provide possibilities for reducing energy consumption in CO_2 desorption. Moreover, the optimization of the hydrogen concentration suggests, by analogy, that there exists an optimum synergy angle to desorb the maximum amount of CO_2 absorbed in monoethanolamine- (MEA-) rich solution. In addition, pinch analysis of CO_2 emissions has provided a promising approach to investigate the CO_2 capture system by the intensification method,[25] which gives us more confidence to pursue better performance using the synergy pinch theory. Based on the information discussed above, the synergy pinch method was applied in this work to analyze the desorption process to seek the regeneration potential at the synergy pinch point or close to it.

In this article, a two-dimensional two-phase flow desorption model is first established to specify the internal fluid flow and mass and heat transfer in the stripper. Attempts are then made to incorporate the gas- and liquid-phase interactive effects and radial variations. Based on the resulting model, enhancement of mass and heat transfer by the presented synergy pinch is investigated in a stripper. It is expected that the synergy pinch theory will demonstrate performance improvement. To pursue this goal, the basic desorption model for the synergy pinch analysis is given first.

2. DESORPTION MODEL

In contrast to the case for absorption, the assumptions for the desorption process are given as follows.

(1) The total equilibrium pressure of the liquid phase is the sum of vapor pressures in the two phases.
(2) Both the vapor and liquid phases are ideally mixed.
(3) The liquid is incompressible.
(4) The liquid and gas phases are each assumed to be continuous.
(5) Two-dimensional mass, energy, and concentration balances for the liquid and gas phases are applied.
(6) The amine is not vaporized.

Based on these assumptions, a mathematical model was developed that consists of the following equations:

liquid-phase continuity equation

$$\nabla\cdot\rho hU = N \tag{1}$$

The amount of CO_2 in the liquid phase, N, was determined by reaction kinetics and equilibrium data in the literature.[8,10−14]

liquid-phase momentum equation

$$\nabla\cdot\rho hUU - \nabla\cdot h\mu_{\text{eff}}\left[\nabla U + (\nabla U)^{\text{T}} - \frac{2}{3}\nabla\cdot UI\right] = -h\nabla p + F \tag{2}$$

The drag force and body force involved in F were developed by correlations in the absorption description.[12−14]

liquid-phase energy equation

$$\nabla\cdot\rho hUH = \nabla\cdot\nabla(\rho h\alpha_{\text{eff}}H) + Q \tag{3}$$

The energy source term was correlated with the amount of CO_2 and the reaction heat.[8]

liquid-phase concentration equation

$$\nabla\cdot\rho hUC = \nabla\cdot\nabla(\rho hD_{\text{eff}}C) + S \tag{4}$$

The liquid-phase concentration varies with the amount of CO_2 and, thus, is a function of N.[8,12,14]

gas-phase continuity equation

$$\nabla\cdot\rho_{\text{g}}h_{\text{g}}U_{\text{g}} = -N \tag{5}$$

gas-phase momentum equation

$$\nabla\cdot\rho_{\text{g}}h_{\text{g}}U_{\text{g}}U_{\text{g}} - \nabla\cdot h_{\text{g}}\mu_{\text{eff g}}\left(\nabla U_{\text{g}} + (\nabla U_{\text{g}})^{\text{T}} - \frac{2}{3}\nabla\cdot U_{\text{g}}I\right) = -h_{\text{g}}\nabla p + F_{\text{g}} \tag{6}$$

gas-phase energy equation

$$\nabla\cdot\rho_g h_g U_g H_g = \nabla\cdot\nabla(\rho_g h_g \alpha_{effg} H_g) + Q_g \quad (7)$$

gas-phase concentration equation

$$\nabla\cdot\rho_g h_g U_g Y = \nabla\cdot\nabla(\rho_g h_g D_{effg} Y) + S_g \quad (8)$$

The enthalpies of the liquid and gas phases in eqs 3 and 7 were correlated with the temperature and thermal capacity.[26−29] The gas-phase source terms (F_g, Q_g, and S_g) were established by revising the relevant liquid-phase source terms. The interface drag force calculation was developed by the pressure drop model in a countercurrent packed column.[30]

The turbulent diffusivity was calculated as

$$D_t = C_0 k\left(\frac{k}{\varepsilon}\right)^{1/2} \quad (9)$$

and the turbulent viscosity is given by

$$\mu_t = \rho C_\mu \frac{k^2}{\varepsilon} \quad (10)$$

The effective parameters ϕ_{eff}, representing diffusivity, viscosity, and thermal diffusivity, were obtained from the equation

$$\phi_{eff} = \phi + \phi_t \quad (11)$$

Following the desorption model above, the important energy performance is presented in terms of energy consumption per unit. The unified energy model is capable of specifying the regeneration energy consumption without the assumptions used in empirical correlations. The detailed configuration is given as follows.

The regeneration energy consumption is defined as

$$\begin{aligned} Q &= Q_S + Q_R + Q_V + Q_F \\ &= \iint_V \frac{L\Delta H_{i,j}}{V}\,dV + \iint_V \frac{N\Delta RH}{V}\,dV + Q_V + Q_F \end{aligned} \quad (12)$$

where Q_S is the sensible heat, Q_R is the required reaction heat, Q_V indicates the energy consumption of vapor, and Q_F is the reflux fluid absorption heat. The sum of the four terms is the regeneration energy consumption.

This model indicates the factors of fluid flow, concentration variation, column configuration, and their interactive impacts on regeneration energy consumption. Generally, essential information such as the fluid flow field, concentration field, and temperature field required in synergy pinch theory can be obtained by solving the model. All of the key parameters for synergy pinch theory, including the cosine of the synergy angle, the regeneration amount of CO_2 (N), and the energy consumption (Q), depend on the physical model of desorption.

3. SYNERGY PINCH THEORY

The synergy pinch theory is a process intensification method that integrates field synergy theory with hydrogen pinch theory. Field synergy theory can focus on the physical phenomenon in the desorption process to locate the weak parts of heat transfer, mass transfer, and chemical reaction. Hydrogen pinch theory provides a simple optimization method for CO_2 desorption because of its ability to minimize utility in the hydrogen system. Therefore, synergy pinch is applied to produce a feasible optimization condition when various fields are synergized in CO_2 desorption. Compared with classical parameter optimization, this theory exhibits global optimization characteristics because all of the physical fields are involved. The key parameter is the synergy angle, which can correlate the various phenomena,[12−14] given by

$$\cos\theta = \frac{U\cdot\nabla\phi}{|U||\nabla\phi|} \quad (13)$$

where the variable ϕ stands for velocity, temperature, and concentration in the respective models.

Similarly to the minimization of surplus hydrogen in the chemical hydrogen system, synergy pinch analysis can be carried out to minimize the amount of surplus CO_2 between the liquid phase and gas phase in the desorption process. Because the graphical method has been demonstrated to be a simple and effective way to analyze the hydrogen system, efforts were made to establish a synergy pinch graphical method in the CO_2 desorption system. The carbon synergy pinch graph is constructed to implement the optimization process and to obtain the optimum synergy angle, at which the largest amount of regeneration CO_2 can be obtained, as shown in Figure 2. The energy synergy pinch graph can ascertain the optimum regeneration energy consumption based on the synergy condition in Figure 3. The two graphs can be used to assess whether the regeneration process is at optimal conditions.

Based on eqs 1 and 4, the area composed of the coordinates and the carbon source or sink profile in Figure 2 is the impact of the fluid flow between the two phases on the regeneration amount, as calculated in the equation

$$(\rho hU\cdot\nabla C)\frac{\nabla\cdot hU}{h|U||\nabla C|} = N\cos\theta \quad (14)$$

Equation 14 shows that the area is the regeneration amount of CO_2 induced by variations in the liquid MEA solution concentration. In the gas phase of CO_2 and steam, the area represents the amount of CO_2 caused by variation of the gas fraction (Y), substituting the MEA concentration (C) gradient in eq 14. The resulting area differences represent the degree of synergy between carbon source and sink.

By referencing hydrogen pinch theory, the carbon source and carbon sink are set as CO_2 in the gas phase and a rich solution of MEA, respectively. Figure 2 shows the amount of CO_2 in the desorption process in the horizontal direction, representing the amount desorbed from MEA solution and the quantity existing in the steam phase. The cosine of the synergy angle is set as a vertical variable that is in descending order by the field synergy distributions. The difference between the two points in the horizontal direction is the amount of CO_2 regenerated. Its function is equal to the cosine of the synergy angle, which is described as the line segment parallel to the horizontal coordinate.

The area defined in Figure 3 is the energy requirement caused by fluid flow velocity variation (convection heat transfer). The energy synergy pinch graph (Figure 3) is established in the independent variable of regeneration energy consumption. Its vertical variable is the same cosine of the synergy angle as in the carbon synergy pinch graph. The energy source and sink profiles consist of groups of line segments, each of which represents the cosine value of the synergy angle versus the horizontal difference between the two points of the regeneration energy consumption.

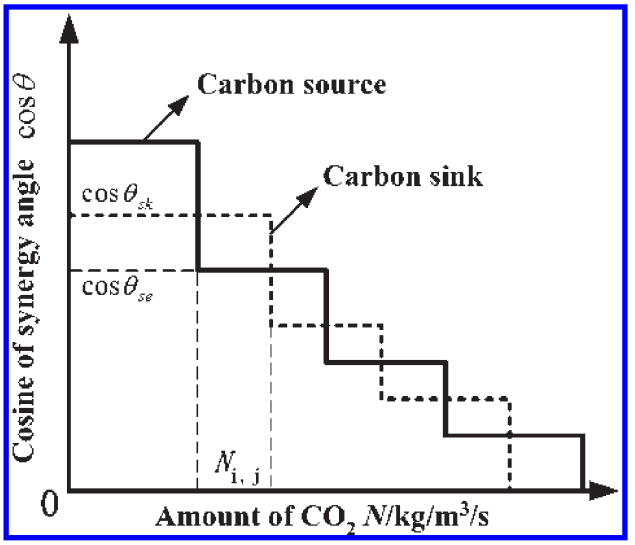

Figure 2. Cosine of the synergy angle for the carbon source and carbon sink.

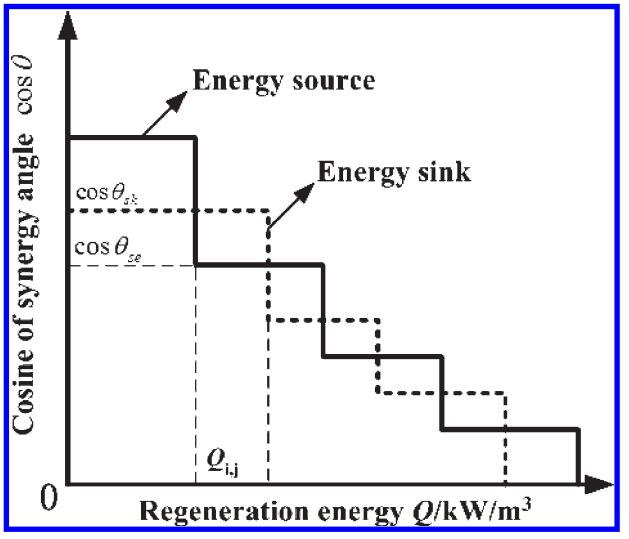

Figure 3. Cosine of the synergy angle for the energy source and energy sink.

After identifying the source and sink terms, the synergy pinch is implemented as follows: First, two key parameters (SAC and SAE) are deduced based on the carbon and energy synergy pinch graphs. The surplus amount of CO_2 (SAC) is defined as

$$\mathrm{SAC} = (\cos\theta_{\mathrm{se}} - \cos\theta_{\mathrm{sk}})N_{i,j} \tag{15}$$

This definition shows the area difference between the carbon source and sink. The following steps determine how to form the curve of SAC: If the SAC is positive, it is drawn along the positive direction of the horizontal axis. Otherwise, it is depicted in the negative direction, as shown in Figure 4. Connecting the points with one line gives the surplus graph. The principle is that the final surplus amount of CO_2 in Figure 4 should be equal to zero if the maximum amount of regenerated CO_2 is produced. The pinch point is formed when the final surplus amount of CO_2 reaches zero. Its arccosine value is the optimum synergy angle that can induce the best synergy between fluid flow and mass transfer.

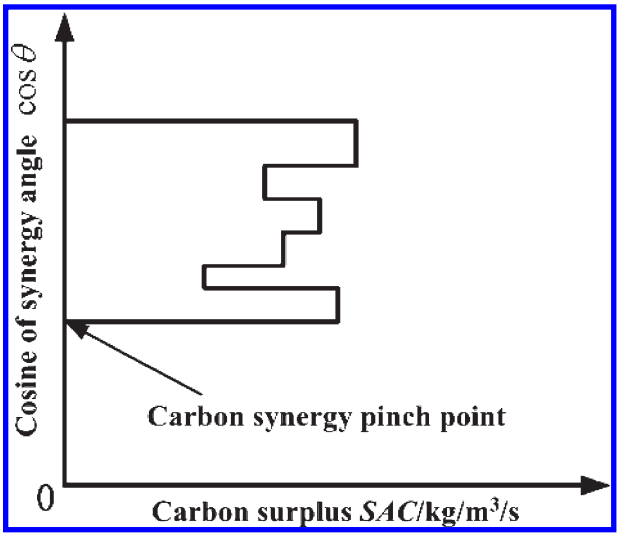

Figure 4. Carbon surplus diagram.

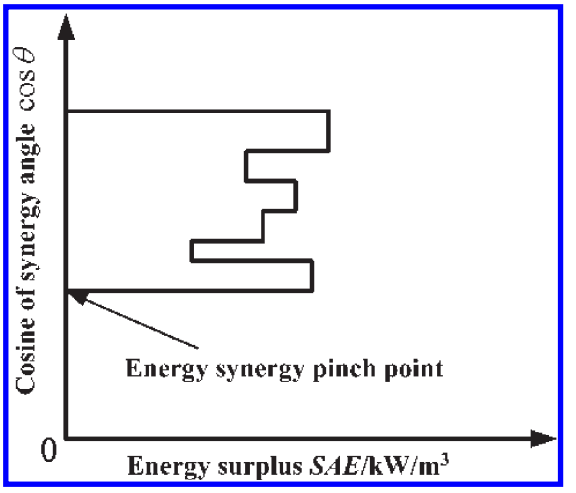

Figure 5. Energy surplus diagram.

The surplus amount of regeneration energy consumption (SAE) is formulated as

$$\mathrm{SAE} = (\cos\theta_{\mathrm{se}} - \cos\theta_{\mathrm{sk}})Q_{i,j} \tag{16}$$

The surplus graph for the regeneration energy consumption is composed of the quantity of horizontal SAE and the cosine of the synergy angle on the vertical axis, as shown in Figure 5. The SAE value is depicted positively when it is greater than zero, and otherwise, it is drawn along the horizontal direction negatively. The pinch point can be identified when the value of SAE is zero, where the minimum regeneration energy is achieved with the optimum synergy angle.

However, in most practical processes, the values of SAC and SAE might approach zero, but it is difficult for them to reach zero. Thus, the principle is that the lower the surplus, the more efficient the synergy pinch effect. If the synergy angles in the source and sink terms deviate significantly, effective measures should be taken to adjust them to obtain a reasonable surplus of carbon and energy. Structural retrofitting of the stripper can be one promising approach.

dx.doi.org/10.1021/ie2004847 |*Ind. Eng. Chem. Res.* 2011, 50, 13997–14007

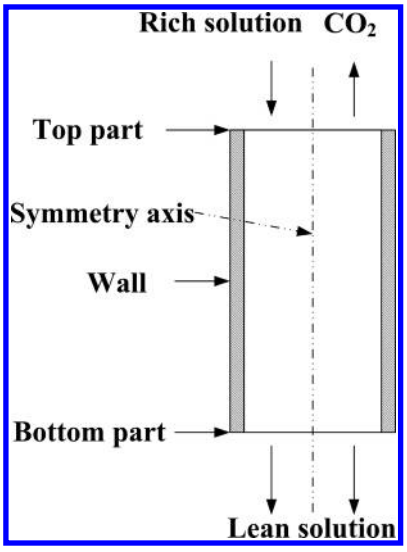

Figure 6. Simplified simulation domain for the thermal regeneration of CO_2.

Based on the pinch points of carbon synergy and energy synergy, there exists a balance between the two optimum synergy angles that can simultaneously achieve the largest amount of regeneration CO_2 and the lowest regeneration energy consumption. Moreover, the field with synergy angles larger than the optimum pinch synergy angle should be adjusted to intensify the process. The entire synergy pinch analysis relies on the numerical simulation results, which should be obtained first.

4. NUMERICAL SIMULATIONS

The numerical simulations were carried out by the finite-volume method (FVM) with a self-developed program. The SIMPLE algorithm was applied in the program to solve the pressure−velocity coupling equations. The additional source term method assured convergence at a mass imbalance of 10^{-3}. The relevant initial and boundary conditions and physical parameters are summarized in the next subsection. Also, a case study is provided necessarily to verify the model.

4.1. Physical Parameters and Boundary Conditions. The equilibrium and reaction heat parameters were employed in the form of correlations with temperature and solution loading.[8] The reaction kinetics was calculated from the concentrations of $MEACOO^-$ and $MEAH^+$, describing the reversible process.[10] The viscosity and density are both cited in Cheng et al.'s contribution to the physical properties of MEA solution.[27] For the diffusion process, the analogous results were applied in the desorption of CO_2.[31,32] The effective interface area was correlated with the packing area, surface tension, and viscosity.[33]

The relevant boundary conditions are presented as follows:

(1) The velocity inlet boundary at the top of the column was set as $u = u_{avg}$, $v_{in} = 0$, $H = H_{in}$, $Y = Y_{in}$, $k_{in} = 0.005u_{in}^2$, $\varepsilon_{in} = 0.09k_{in}^{1.5}/d_y$, and $d_y = 4\gamma_\infty/[a(1 - \gamma_\infty)]$.

(2) The outflow of the boundary was assumed to be fully developed, so the equation $\partial\phi/\partial x = 0$ holds.

(3) At the axis, all variables were assumed to be mathematically symmetric; therefore, $\partial\phi/\partial r = 0$ when $r = 0$.

(4) At the wall, nonslip conditions were applied.

A simplified simulation domain is depicted in Figure 6. Because the stripper is symmetric, one-half of the column was chosen as the computational zone. A uniform mesh was employed in the numerical simulation. To satisfy the grid independence of the calculations, the simulations were conducted with meshes of 80 × 20, 125 × 25, and 140 × 30. The deviation among the three kinds of meshes was within 0.5%. Therefore, the mesh of 125 × 25 was considered to be reasonable.

Table 1. Operating Conditions and Stripper Structure

parameter	value
internal diameter (m)	0.1
packing height (m)	3.89
packing area (m^2/m^3)	250
channel base (m)	0.0241
channel side (m)	0.017
crimp height (m)	0.0119

4.2. Model Validation. To test the proposed model, the solution temperature and CO_2 partial pressure were predicted in the stripper. Sulzer Mellapak 250Y was chosen as the packing in the stripper, whose properties are listed in Table 1.

According to the operating conditions and properties and structure of the stripper, the predicted temperature profile is compared with the results of run 2 in stripper experiments in Table 2.[9] The computed pressure was plotted with the measured pressure of run 7 in the stripper experiments in Table 2.[9] The MEA lean solvent from the stripper had a weight fraction of 30%.

As shown in Figure 7, the temperature of the liquid solution fits the experimental data for the stripper. The largest deviation is produced around the region at the top of the stripper. The reason might be that the reflux liquid heated the liquid to some extent, whereas the impact of reflux on the liquid temperature was ignored in the simulation. Meanwhile, the numerical solution inevitably causes some uncertainties. Thus, the model can reasonably reflect the liquid temperature distribution in the stripper.

The predicted CO_2 partial pressure is also compared with the measuring data (see Figure 8). The two-dimensional pressure distributions are averaged in the radial direction in the validation process. It is certain that the model predicted the partial pressure precisely along the stripper, as little deviation can be observed in Figure 8.

Based on the results of the comparison, the model is deemed satisfactory for describing the CO_2 desorption process. Thus, the synergy pinch analysis can be discussed according to the synergy pinch theory described in section 3.

5. SYNERGY PINCH DISCUSSION

As indicated in section 3, the field synergy distribution should first be simulated. With field synergy analysis, the physical process state presented by key parameters of cosines of the synergy angle can be obtained. The synergy angle can indicate whether the desorption process is good. It is regarded as the cornerstone for the discussion of synergy pinch. Therefore, the specification of field synergy is given and summarized.

5.1. Regeneration Field Synergy. The field synergy among fluid flow, temperature, solution concentration and gas fraction is investigated in the regeneration of CO_2. The temperature and concentration fields for the gas and liquid phase are the main focuses because of their direct connections to the amount of CO_2 and regeneration energy consumption.

Table 2. Operating Conditions for Runs 2 and 7 in Stripper Experiments[9]

	rich solution inlet		poor solution outlet					
run	temperature (K)	loading (mol/mol)	temperature (K)	loading (mol/mol)	MEA concentration ($kmol/m^3$)	CO_2 flow rate (kg/s)	liquid flux [$m^3/(m^2/s)$]	pressure (MPa)
2	388.15	0.315	394.15	0.248	5.0	0.0014	0.0021	0.197
7	388.15	0.295	391.15	0.276	4.7	0.0013	0.0032	0.2005

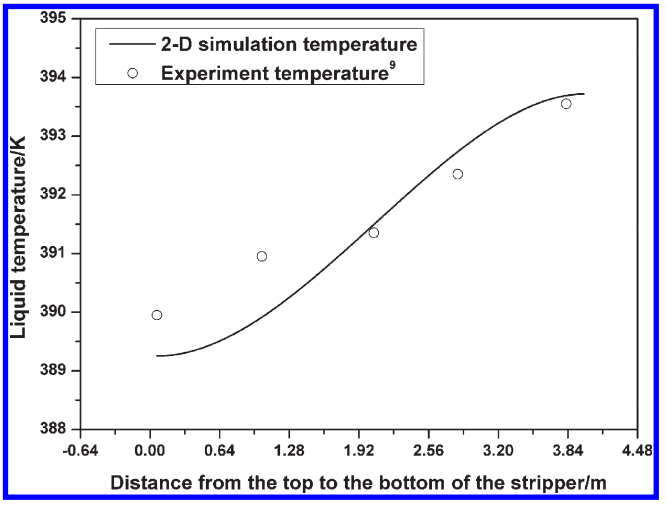

Figure 7. Liquid temperature distribution profile in the stripper.

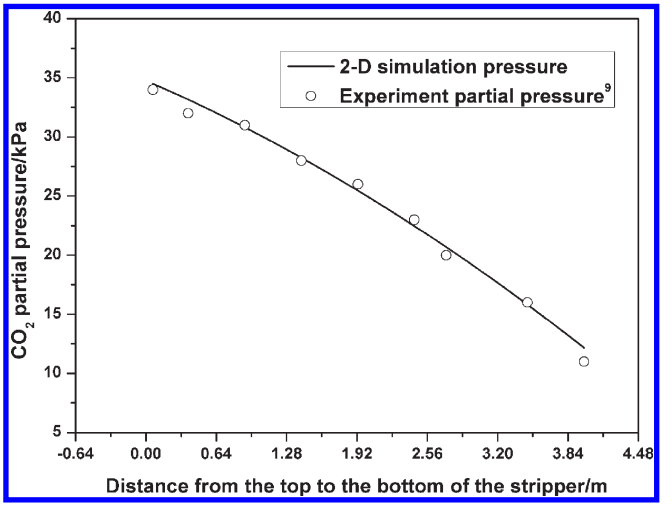

Figure 8. Partial pressure of CO_2 in the desorption process.

5.1.1. Temperature Synergy Distribution. The temperature synergy distribution is shown in Figure 9a, which demonstrates a good synergy between fluid flow and heat transfer in most parts of the stripper with a synergy angle of about 8°. The central zone synergy, with a synergy angle of 85°, is not as good as that in the other parts. This indicates that the fluid flow field and temperature field are not synergized properly because of a larger drag force between the two phases in the center. Therefore, the intensification should be focused in the central part to reduce its synergy angle. Increasing solution flow velocity is supposed to reduce the force. Moreover, enhancing the fluid flow in the central area can intensify the heat transfer between the MEA solution and the steam. This can be realized if the interface force between the MEA solution and the steam phase is reduced by achieving synergy pinch.

5.1.2. MEA Concentration Synergy Distribution. As shown in Figure 9b, the synergy between the fluid flow and the MEA concentration is inadequate for the desired process because a synergy angle of 85° is distributed in most zones, except the better central part. In this sense, the fluid flow velocity is almost perpendicular to the MEA concentration gradient. Apparently, this contributes to the fact that the concentration field is not intensified significantly by flow field under this circumstance. Compared with the synergy angle distribution in Figure 9a, it is obvious that the worse synergy has been produced between the fluid flow and MEA concentration. However, the synergy balance should be kept between heat transfer and mass transfer because of the opposite impact of fluid flow on the temperature and concentration. This goal can be achieved by reducing the carbon surplus (SAC) and the energy surplus (SAE). In other words, the fluid flow should be adjusted to harmonize heat transfer with mass transfer based on the synergy pinch analysis.

5.1.3. Regeneration CO_2 Concentration Synergy Distribution. The synergy between the fluid flow and the CO_2 concentration distribution has been identified as the best among the three field synergy distributions as shown in Figure 9c. The average synergy angle is about 45°. The reason is that the gas-phase velocity is large enough to enhance the mass transfer in the stripper. Compared with slow solution flow, gas-phase flow produces a much more significant impact on gas diffusion. However, the synergy effect should be improved in the central region to reduce its synergy angle, as well as in the top part. This can be achieved by increasing the gas-phase velocity with a slight decrease of the flux area in the stripper based on the synergy pinch principle.

5.2. Synergy Pinch Analysis. All three kinds of field adjustments to achieve the optimum performance can be interactive in the stripper. The synergy pinch can provide a benchmark to synergize the three fields. Thus, the overall synergy effect improvement can be achieved by satisfying the synergy pinch principle, as described in the next section.

5.2.1. Carbon Source and Sink. Because synergy angles have already been presented in Figure 9, the carbon source and carbon sink (see Figure 10) can be directly obtained by following the procedure in section 3. As expected, a great difference has been shown between the synergy effect of carbon source and carbon sink. The CO_2 regenerated term is defined as carbon source while the MEA solution is set as carbon sink. The carbon source exhibits better synergy with the cosine of synergy angle in the range of 0.7 and 0.9, which is close to 1. However, the worst synergy between the fluid flow fields and MEA solution concentration fields has resulted in about 0.1 of the cosine of synergy angle for the carbon sink. This indicates that the MEA fluid flow should be improved to coordinate its synergy with MEA solution concentration field. It also proves that wall flow has significantly

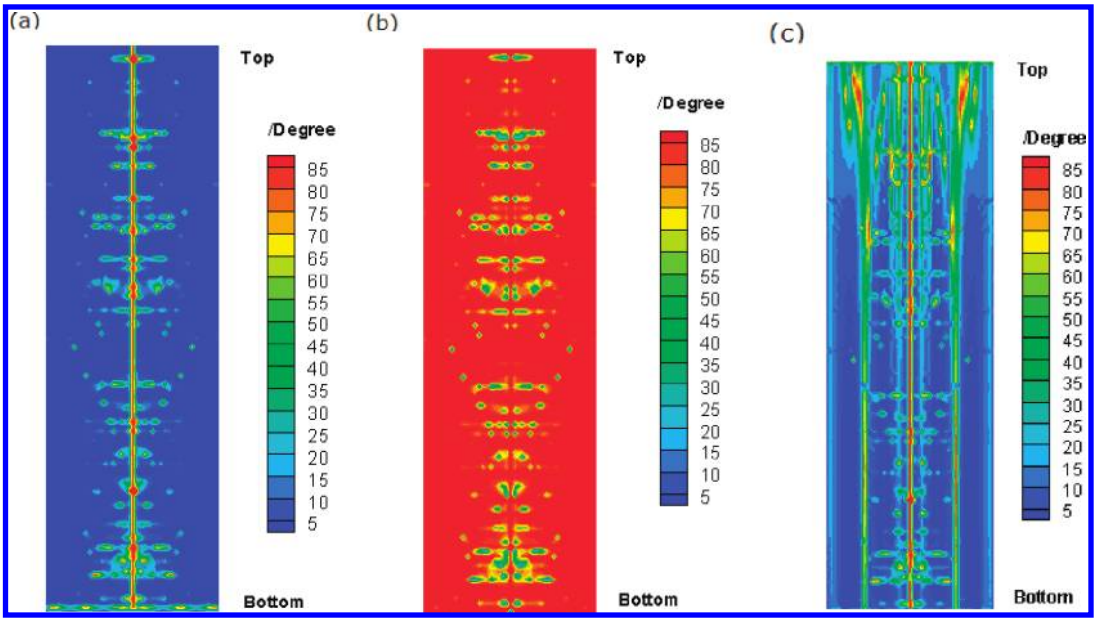

Figure 9. Synergy angles between the velocity and gradient of the (a) temperature, (b) MEA concentration, and (c) CO_2 fraction.

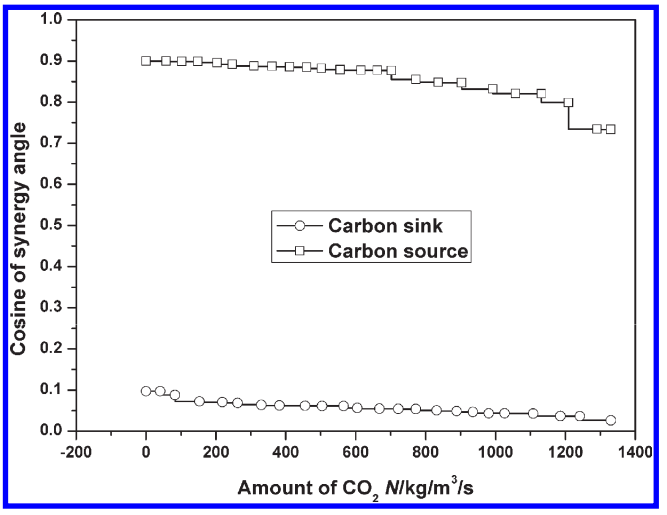

Figure 10. Carbon source and sink diagram in the desorption of CO_2.

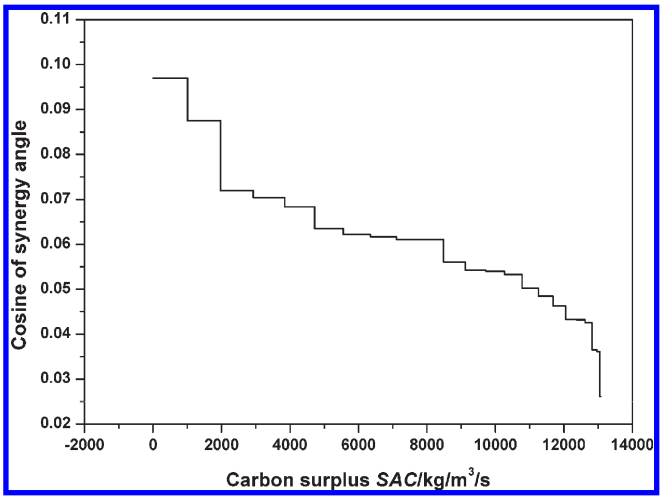

Figure 11. Carbon surplus diagram in the desorption of CO_2.

affected carbon sink. However, this is just a little setback for the carbon source. Therefore, it is possible to reduce the synergy angle to balance the fluid flow impact on the liquid MEA and gas-phase variation, which is supposed to reduce the interface force between the two phases.

5.2.2. Carbon Surplus Graph. By combining the carbon source and carbon sink in Figure 10, the carbon surplus diagram was constructed (Figure 11). The carbon surplus (SAC) at the largest synergy angle (about 0.025 cosine value) is about 1.3×10^4 kg/(m^3/s), which is much greater than zero. Thus, according to the synergy pinch principle, measures should be taken to reduce the SAC to ensure that it is close to zero for achieving better synergy effect in the regeneration system. Because CO_2 desorption is a multiphysical process, the synergy pinch analysis of energy should be considered, too. Only when the carbon/energy source and sink simultaneously reach reasonable synergies can the CO_2 desorption be deemed effective. In this sense, significantly efficient desorption can achieve large amounts of regeneration CO_2 at the expense of low energy consumption.

5.2.3. Energy Source and Sink. The basic synergy angles between fluid flow field and temperature field can be deduced by field synergy analysis. Similarly to the carbon source and sink definition, the gas phase has been defined as the energy sink, whereas the MEA solution has been defined as the energy source (see Figure 12). In the lower energy consumption zone, less than 2.0×10^6 kW/m^3, the synergy is not good because of the large deviation between the cosines of the synergy angles for the source and sink terms. Under these circumstances, the deviation is attributed to a stronger heat-transfer impact on the MEA solution than in the gas phase. Hence, the interface heat-transfer resistance should be reduced to remove the synergy pinch obstacle.

5.2.4. Energy Surplus Graph. As shown in Figure 13, the energy source and energy sink produced the energy surplus. The energy surplus SAE (at a cosine value of 0.73) is 2.30×10^6 kW/m^3, which is much greater than zero. By the synergy pinch

dx.doi.org/10.1021/ie2004847 |*Ind. Eng. Chem. Res.* 2011, 50, 13997–14007

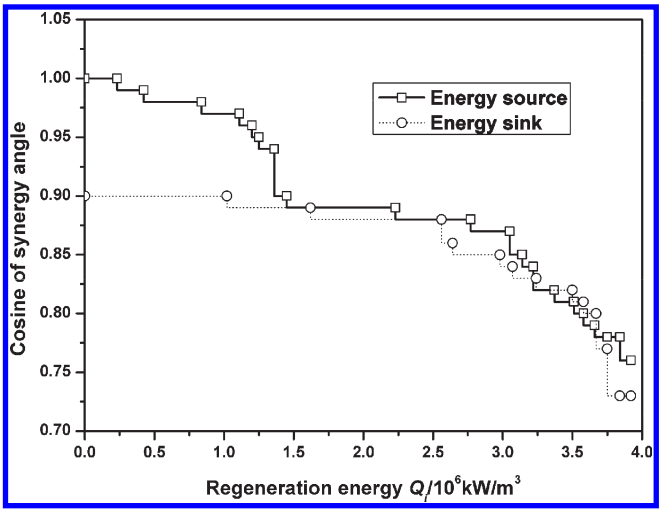

Figure 12. Energy source and sink diagram in the desorption of CO_2.

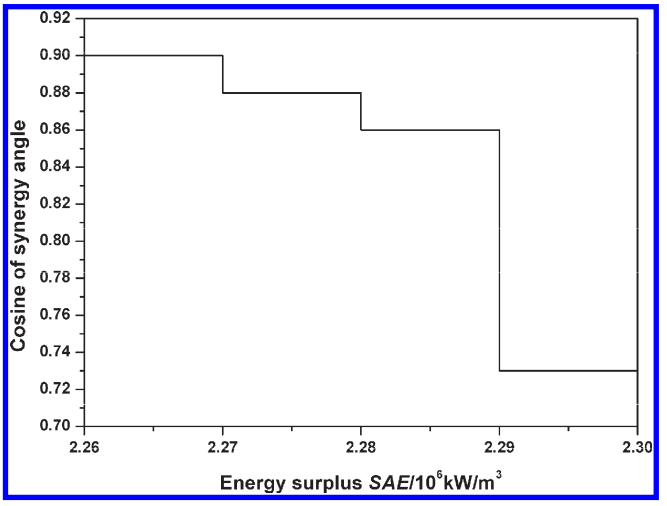

Figure 13. Energy surplus diagram in the desorption of CO_2.

principle, the synergy angle should be adjusted to synergize the heat transfer between the two phases. It is anticipated that the fluid flow can be enhanced to reduce the heat-transfer resistance in light of the synergy pinch analysis. The guideline is that the energy surplus must be close or equal to zero.

In summary, the synergy pinch analysis results suggest that the fluid flow has a significant impact on the mass and heat transfer. To reduce the values of SAC and SAE so as to ensure the formation or approximate formation of a synergy pinch point, a fin internal stripper is proposed in the next section to improve the fluid flow. The retrofit in the structure focuses on increasing the fluid flow velocity to synergize the fluid flow field and concentration field.

6. STRUCTURE RETROFIT FOR A STRIPPER

According to the synergy pinch discussed in the preceding section, the key steps involve improving the fluid flow to achieve better synergy. Therefore, the fin internals were designed to reduce the wall flow and increase the velocity in the stripper. The stripper with fin internals is a packed column with three-segment ring inside as described in Figure 14. The distances (H_2) between

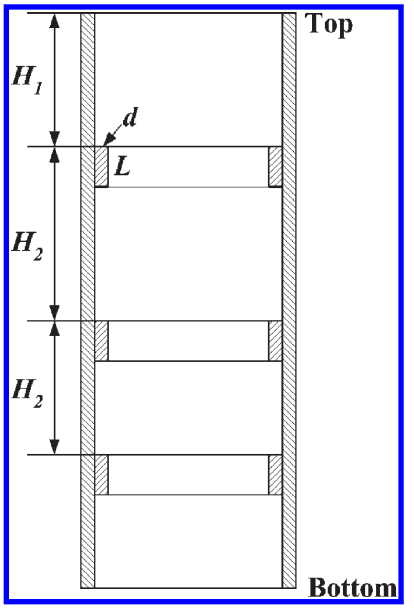

Figure 14. Structural schematic of a stripper with fin internals.

Table 3. Geometrical Characteristics of Internals in the Retrofit Stripper

parameter	value (m)
H_1	0.996
H_2	1.929
d	0.009
L	0.311

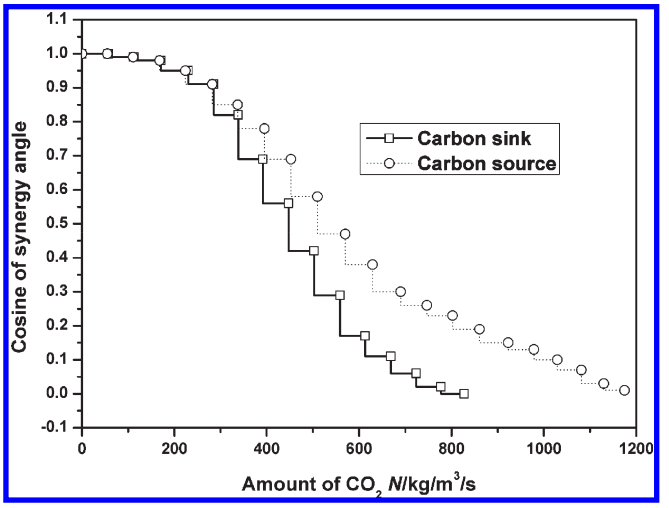

Figure 15. Carbon source and carbon sink diagram for a stripper with fin internals.

pairs of segments are the same, whereas the fin internals' thickness is d, and the height is L. The first segment is set at a distance of H_1 from the top of the stripper. The relevant geometrical parameters are listed in Table 3.

After the fin internals were assembled into the stripper, the synergy pinch method was applied to investigate their effect on the mass and heat transfer. Comparison with a smooth-wall

dx.doi.org/10.1021/ie2004847 |*Ind. Eng. Chem. Res.* 2011, 50, 13997–14007

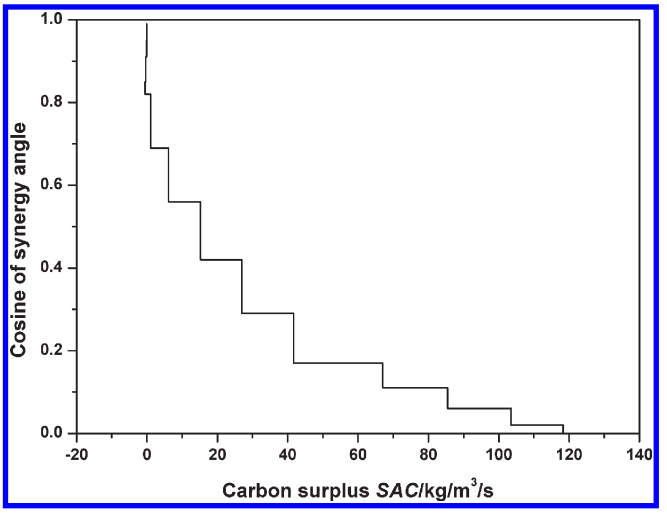

Figure 16. Carbon surplus diagram for a stripper with fin internals.

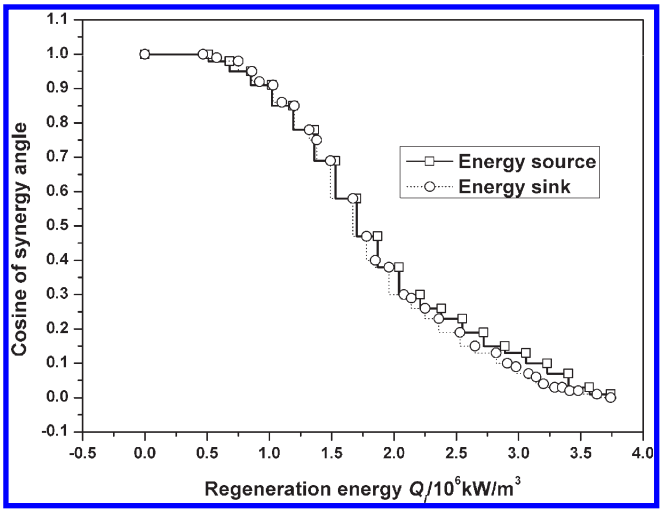

Figure 17. Energy source and sink diagram for a stripper with fin internals.

stripper was carried out to demonstrate its impact. The results are given in the following section.

6.1. Carbon Source and Sink with Retrofit. The carbon source and sink for the stripper with fin internals are depicted in Figure 15. It can be seen that the synergy effect between the carbon sink and carbon source tends to be uniform. A lower deviation for the cosines of the synergy angles was obtained satisfactorily. Compared with that in Figure 10, the small synergy angle differences were produced because the fin internals increased the velocity of the liquid and reduced the synergy angle between the velocity and MEA concentration gradient. Also, the interface force between the two phases decreased as a result of the reduction of the interface velocity difference. Meanwhile, the fin internals also contribute positively to the two-phase flow synergy by mitigating the wall flow phenomenon.

6.2. Carbon Surplus with Retrofit. Figure 16 shows the carbon surplus for the stripper with fin internals according to the carbon source and carbon sink. A synergy angle fluctuation produced a more uniform variation of carbon surplus. Compared with that in Figure 11, the carbon surplus SAC is significantly reduced to 120 kg/m^3/s at the 0.02 cosine of synergy angle, which indicates that the synergy pinch is approached more properly than that in the smooth wall stripper. Thus, according to the synergy pinch principle, the mass transfer is more cooperative between the two phases. The fluid flow has been enhanced by the synergy angle distribution adjustment for the MEA concentration field and gas-phase concentration field. Thus, the retrofit with fin internals is effective for intensifying the desorption process.

6.3. Energy Source and Sink with Retrofit. Likewise, the energy source and sink for stripper with fin internals are predicted in Figure 17. Good performance is observed for the temperature synergy between the solution and vapor phases. The deviation for the cosines of the synergy angles is less than 0.1, and the minimum deviation is zero in the lower energy consumption zone. The uniform synergy angle tendency has been observed because the fin internals in the stripper increases the solution velocity, achieving a better synergy between the fluid flow and heat transfer. It should be noticed that the enhancement mainly affects the lower energy consumption zone. As for the higher energy consumption part, the synergy pinch deviates slightly, but can be considered to be suitable enough because of a slight variation between energy source and sink.

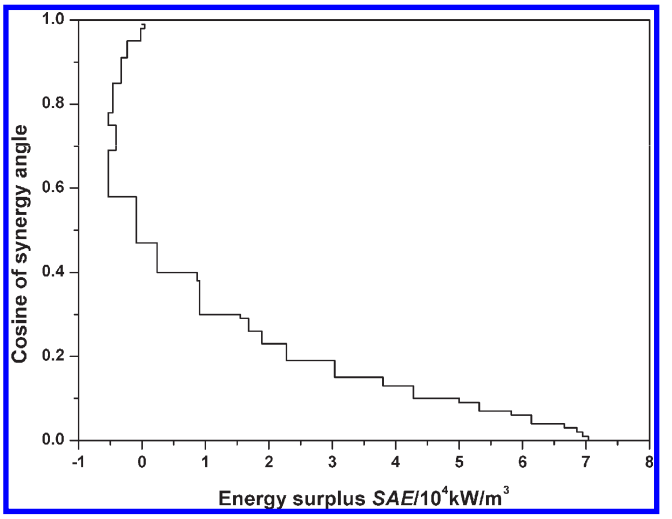

Figure 18. Energy surplus diagram for a stripper with fin internals.

6.4. Energy Surplus with Retrofit. As expected, the energy surplus in Figure 18 shows a significant SAE drop with the contributions of the fin internals. The SAE is observed as about 7×10^4 kW/m^3, only 3% of that in the smooth wall stripper. In this sense, this lower energy surplus demonstrates that the heat transfer resistance has been significantly reduced between the two phases. It must be noted that although the synergy pinch point was not reached, the synergy effect was moderately realized by assembling the fin internals. The drop of both the carbon surplus and the energy surplus demonstrates that a balance between the regeneration of CO_2 and energy conservation has been achieved.

6.5. Performance Assessment. Comparison of the results obtained by synergy pinch analysis can provide the overall impact of fin internals on stripper performance (see Table 4). Generally, the sensible heat, reaction heat, and vapor/reflux energy consumption were all reduced after fin internals were assembled into the stripper. The most significant heat drop was about 25% because the amounts of vapor and reflux fluid were reduced at the top of the stripper. The amount of CO_2 regenerated was almost

Table 4. Performance Comparison between Strippers with Fin Internals and Smooth Walls

stripper	rich liquid loading (mol/mol)	poor liquid loading (mol/mol)	sensible heat (kW)	reaction heat (kW)	vapor/reflux heat (kW)	amount of CO_2 (kg/s)	energy consumption (GJ/t)
smooth walls	0.295	0.276	1399.39	2657.38	4275.6	1.40	5.95
fin internals	0.295	0.276	1348.28	2589.58	3183.1	1.39	5.11
smooth walls	0.457	0.401	1536.95	3755.29	1626.8	1.87	3.7
fin internals	0.457	0.401	1529.04	3465.59	1171.3	1.85	3.33

the same, with a negligible drop of about 1%. This is attributed to the shrinkage of the effective cross-sectional area caused by the fin internals. In accordance with the amount of CO_2 and four parts of heat in Table 4, an energy consumption of 5.11 GJ/t of CO_2 was calculated for the stripper with fin internals at a low average loading of 0.286 mol/mol. With the higher average loading of 0.429 mol/mol, the stripper with fin internals consumed 3.33 GJ/t of CO_2 thermal energy. Compared with energy consumption in the smooth-wall stripper, a 14% energy conservation potential was achieved at a low loading in the stripper with fin internals. As the loading increased, there was a 10% energy conservation potential compared with that in the smooth-wall stripper.

In summary, the stripper with fin internals performed well from the perspective of mass transfer and energy consumption. However, the structure optimization can still be investigated further to reach the synergy pinch point.

7. CONCLUSIONS

A two-dimensional two-phase flow desorption model was established to simulate the regeneration of CO_2 in a packed column. The field synergy distributions located the weak mass and heat transfer in the stripping process. The proposed synergy pinch theory was applied in the regeneration process analysis, which was presented in the form of indexes SAC and SAE. SAC and SAE far from the synergy pinch points, indicating that the synergy angle should be adjusted to achieve the largest amount of regeneration CO_2 and lowest amount of regeneration energy consumption. The designed stripper with fin internals conformed to the synergy pinch principle according to the synergy pinch analysis results. It was concluded that the regeneration amount of CO_2 could be kept constant while the energy consumption could be reduced by 10−14% by fin internals. The results demonstrated that synergy pinch analysis is an effective alternative way to intensify the desorption process.

However, the optimum structure of the stripper can be redesigned further according to synergy pinch optimization to achieve the synergy pinch point where SAC and SAE are zero. This can be carried out by combining the synergy pinch principle with field synergy optimization[12−14] in a future research work.

■ ASSOCIATED CONTENT

Supporting Information. Computation schematic to implement the synergy pinch analysis. This material is available free of charge via the Internet at http://pubs.acs.org.

■ AUTHOR INFORMATION

Corresponding Author

*Tel.: +86-29-8266 0689. Fax: +86-29-8266 8566. E-mail: zhangzx@mail.xjtu.edu.cn.

■ ACKNOWLEDGMENT

Financial support provided by the National Natural Science Foundation of China under Grants 50976090 and 20936004 is gratefully acknowledged. The team also thanks colleagues at Xi'an Jiaotong University for their helpful comments during manuscript preparation.

■ NOMENCLATURE

C = concentration of liquid
C_0 = coefficient
C_μ = coefficient
D = diffusivity, m^2/s
d_y = hydraulic diameter, m
F = source term of the momentum equation, N/m^3
H = enthalpy, kJ/kg
h = liquid volume fraction
I = unit tensor
k = turbulent kinetic energy, m^2/s^2
L = liquid flux, $kg/(m^3\ s)$
N = source term of the continuity equation, $kg/(m^3\ s)$
p = pressure, kPa
Q = source term of the energy equation/energy consumption, kW/m^3
r = radial direction, m
RH = reaction heat, kJ/kg
SAC = carbon surplus, $kg/(m^3\ s)$
SAE = energy surplus, kW/m^3
U = liquid velocity vector, m/s
u = axial velocity, m/s
V = volume, m^3
v = radial velocity, m/s
x = axial direction, m
Y = gas-phase concentration
α = thermal diffusivity, m^2/s
λ = porosity
ρ = density, kg/m^3
μ = viscosity, $kg/(m\ s)$
ε = turbulent dissipation rate, m^2/s^3
ϕ = variable for velocity, temperature, and concentration
θ = synergy angle, deg

Subscripts

avg = average
eff = effective
F = reflux fluid
g = gas phase
i = radial grid position
in = inlet
j = axial grid position
R = reaction heat term
S = sensible heat term
se = source
sk = sink

t = turbulent
V = vapor

REFERENCES

(1) Cornelisse, R.; Beenackers, A. A. C. M.; Beckum, F. P. H. V.; Swaaij, W. P. M. V. Numerical calculation of simultaneous mass transfer of two gases accompanied by complex reversible reactions. *Chem. Eng. Sci.* **1980**, *35*, 1245.

(2) Suenson, M. M.; Georgakls, C.; Evans, L. B. Steady-state and dynamic modeling of a gas absorber−stripper system. *Ind. Eng. Chem. Res. Fund.* **1985**, *24*, 288.

(3) Escobillana, G. P.; Saez, J. A.; Perez-correa, J. R.; Neuburg, H. J. Behaviour of absorption/stripping columns for the CO_2−MEA system; Modelling and experiments. *Can. J. Chem. Eng.* **1991**, *69*, 969.

(4) Alatiqi, I.; Sabri, M. F.; Bouhamra, W.; Alper, E. Steady-state rate-based modelling for CO_2/amine absorption−desorption systems. *Gas Sep. Purif.* **1994**, *8*, 3.

(5) Iliuta, I.; Petre, C. F.; Larachi, F. Hydrodynamic continuum model for two-phase flow structured-packing-containing columns. *Chem. Eng. Sci.* **2004**, *59*, 879.

(6) Budzianowski, W.; Koziol, A. Stripping of ammonia from aqueous solutions in the presence of carbon dioxide: Eeffect of negative enhancement of mass transfer. *Chem. Eng. Res. Des.* **2005**, *83*, 196.

(7) Tobiesen, F. A.; Svendsen, H. F. Study of a modified amine-based regeneration unit. *Ind. Eng. Chem. Res.* **2006**, *45*, 2489.

(8) Oyenekan, B. A. Modeling of strippers for CO_2 capture by aqueous amines. Ph.D Thesis, The University of Texas at Austin, Austin, TX, 2007.

(9) Tobiesen, F. A.; Juliussen, O.; Svendsen, H. F. Experimental validation of a rigorous desorber model for CO_2 post-combustion capture. *Chem. Eng. Sci.* **2008**, *63*, 2641.

(10) Plaza, J. M.; Wagener, D. V.; Rochelle, G. T. Modeling CO_2 capture with aqueous monoethanolamine. *Int. J. Greenhouse Gas Control* **2010**, *4*, 161.

(11) Huepen, B.; Kenig, E. Y. Rigorous modeling and simulation of an absorption−stripping loop for the removal of acid gases. *Ind. Eng. Chem. Res.* **2010**, *49*, 772.

(12) Yu, Y. S.; Li, Y.; Lu, H. F.; Yan, L. W.; Zhang, Z. X.; Wang, G. X.; Rudolph, V. Multi-field synergy study of CO_2 capture process by chemical absorption. *Chem. Eng. Sci.* **2010**, *65*, 3279.

(13) Yu, Y. S.; Yan, L. W.; Li, Y.; Zhang, Z. X.; Feng, X. Field synergy optimization for CO_2 capture process by chemical absorption. In *Proceedings of the 5th International Symposium on Design, Operation and Control of Chemical Processes (PSE ASIA 2010)*; National University of Singapore: Singapore, 2010; p 259.

(14) Yu, Y. S.; Li, Y.; Lu, H. F.; Yan, L. W.; Zhang, Z. X. Performance improvement for chemical absorption of CO_2 by global field synergy optimization. *Int. J. Greenhouse Gas Control* **2011**, *5*, 649.

(15) Alves, J. Analysis and design of refinery hydrogen systems. Ph.D Thesis, UMIST, Manchester, U.K., 1999.

(16) Hallale, N.; Liu, F. Refinery hydrogen management for clean fuels production. *Adv. Environ. Res.* **2001**, *6*, 81.

(17) Feng, X.; Seider, W. D. A new structure and design methodology for water networks. *Ind. Eng. Chem. Res.* **2001**, *40*, 6140.

(18) Bealing, C.; Hutton, D. Hydrogen-pinch analysis. *Chem. Eng.* **2002**, *109*, 56.

(19) Alves, J. J.; Towler, G. P. Analysis of refinery hydrogen distribution systems. *Ind. Eng. Chem. Res.* **2002**, *41*, 5759.

(20) Wang, B.; Feng, X.; Zhang, Z. X. A design methodology for multiple-contaminant water networks with single internal water main. *Comput. Chem. Eng.* **2003**, *27*, 903.

(21) Zagoria, A.; Huycke, R. Refinery hydrogen management-the big picture. *Hydrocarbon Process.* **2003**, *82*, 41.

(22) Castro, P.; Matos, H.; Fernandes, M. C. Improvements for mass-exchange networks design. *Chem. Eng. Sci.* **1999**, *54*, 1649.

(23) Liu, F.; Zhang, N. Strategy of purifier selection and integration in hydrogen networks. *Chem. Eng. Res. Des.* **2004**, *82*, 1315.

(24) Zhao, Z. H.; Liu, G. L.; Feng, X. New graphical method for the integration of hydrogen distribution systems. *Ind. Eng. Chem. Res.* **2006**, *45*, 6512.

(25) Crilly, D.; Zhelev, T. Emissions targeting and planning: an application of CO_2 emissions pinch analysis (CEPA) to the Irish electricity generation sector. *Energy* **2008**, *33*, 1498.

(26) Reid, R. C.; Prausnitz, J. M.; Poling, B. E. *The Properties of Gases and Liquids*, 4th ed.; McGraw-Hill Book Co: New York, 1987.

(27) Cheng, S.; Meisen, A.; Chakma, A. Predict amine solution properties accurately. *Hydrocarbon Process.* **1996**, *75* (2), 81.

(28) Weiland, R. H.; Dingman, J. C.; Cronin, D. B.; Browning, G. J. Density and viscosity of some partially carbonated aqueous alkanolamine solutions and their blends. *J. Chem. Eng. Data* **1998**, *43*, 378.

(29) Tobiesen, F. A.; Svendsen, H. F. Experimental validation of a rigorous absorber model for CO_2 post combustion capture. *AIChE J.* **2007**, *53*, 846.

(30) Stichlmair, J.; Bravo, J. L.; Fair, J. R. General model for prediction of pressure drop and capacity of countercurrent gas/liquid packed columns. *Gas Sep. Purif.* **1989**, *3*, 19.

(31) Verseeg, G. F.; Vanswaaij, W. P. M. On the kinetics between CO_2 and alkanolamines both in aqueous and non-aqueous solutions. 1. Primary and secondary amines. *Chem. Eng. Sci.* **1988**, *43*, 573.

(32) Snijder, E. D.; Teriele, M. J. M.; Versteeg, G. F.; Vanswaaij, W. P. M. Diffusion coefficients of several aqueous alkanolamine solutions. *J. Chem. Eng. Data* **1993**, *38*, 475.

(33) Tsai, R. E.; Seibert, A. F.; Eldridge, R. B.; Rochelle, G. T. Influence of viscosity and surface tension on the effective mass transfer area of structured packing. *Energy Proc.* **2009**, *1*, 1197.